Research Square

Preprints are preliminary reports that have not undergone peer review.
They should not be considered conclusive, used to inform clinical practice,
or referenced by the media as validated information.

# Adaptive Mesh Refinement (h-Adaptive FEM) for High-Fidelity Thermal Simulation of Microchip Cooling Systems

**Desta Sodano**

desta.sodano@iitg.ac.in

Wolkite University

**Research Article**

**Keywords:** h-adaptive FEM, Poisson equation, adaptive mesh refinement, thermal analysis, microchip cooling, a posteriori error estimation

**Posted Date:** April 1st, 2026

**DOI:** https://doi.org/10.21203/rs.3.rs-9156117/v1

**License:** This work is licensed under a Creative Commons Attribution 4.0 International License.
Read Full License

**Additional Declarations:** No competing interests reported.

# Adaptive Mesh Refinement (h-Adaptive FEM) for High-Fidelity Thermal Simulation of Microchip Cooling Systems

**Desta Sodano Seiso**[1]

[1]**Department of Mathematics, College of Natural and Computational Sciences, Wolkite University, Wolkite, Ethiopia**

**Email: desta.sodano@iitg.ac.in**

**Correspondence:**

**Email: destasodano201@2gmail.com**

## Abstract

This paper presents an h-adaptive finite element method (FEM) for solving the two-dimensional Poisson equation, with application to steady-state heat conduction in microelectronic chips. The governing model captures localized heating generated by high-power components, while fixed boundary temperatures represent heat sink conditions. An a posteriori error estimator based on nodal variation is employed to guide adaptive mesh refinement in regions with steep temperature gradients. Linear triangular (P1) elements are utilized, and localized refinement enables accurate resolution of thermal hotspots while maintaining computational efficiency. Numerical results demonstrate rapid convergence and effective concentration of computational resources near heat sources, indicating that the proposed method is well-suited for efficient thermal analysis in microchip design.

Keywords: h-adaptive FEM; Poisson equation; adaptive mesh refinement; thermal analysis; microchip cooling; a posteriori error estimation

UNDER PEER REVIEW

## 1. Introduction

The relentless advancement of semiconductor technology has led to dramatic miniaturization of electronic components, enabling unprecedented levels of performance and integration density. However, this progress comes at a cost: as device dimensions shrink and clock speeds increase, power densities have risen significantly, resulting in localized thermal hotspots that can severely impact both the performance and reliability of microelectronic systems [1-3].

In particular, microprocessors, graphics processing units (GPUs), and system-on-chip (SoC) devices often exhibit non-uniform power dissipation, where certain regions-such as computational cores or memory blocks-generate significantly more heat than others [4,5]. These thermal hotspots can lead to local overheating, thermal-induced mechanical stress, and even device failure if not properly managed. Therefore, accurate thermal modelling and simulation are essential tools in the design and optimization of modern cooling strategies [6,7].

Numerical simulation plays a crucial role in predicting and mitigating these thermal effects. Among available numerical techniques, the Finite Element Method (FEM) offers flexibility in handling complex geometries, heterogeneous materials, and non-uniform boundary conditions,

making it particularly suitable for modelling heat transfer in microelectronics [8,9]. In this work, we present an h-adaptive finite element method (FEM) for solving the steady-state heat conduction equation, motivated by applications in microchip cooling. The governing equation models localized heating due to high-power components on a chip, with fixed boundary temperatures simulating heat sink attachment. A posteriori error estimation based on nodal variation drives mesh refinement around regions of steep temperature gradients. Linear triangular ( $P_1$) elements are used, and local mesh refinement ensures accurate resolution of thermal hotspots while minimizing computational cost.

Our implementation demonstrates how adaptive FEM can be effectively used in microchip thermal analysis, enabling fast and accurate simulations for real-world design scenarios.

### 1.1 Motivation: Thermal Challenges in Microchip Design

Modern microchips operate under increasingly stringent thermal constraints. As feature sizes drop below 5 nm and transistor counts rise into the billions, hotspot temperatures can exceed safe operational limits, leading to:

1. Reduced device lifespan
2. Increased leakage currents
3. Throttling of performance
4. Mechanical warping or delamination [10]

To address these challenges, engineers must develop efficient cooling solutions, such as:

a. Heat sinks and heat spreaders
b. Liquid cooling channels
c. Phase-change materials
d. Thermoelectric coolers

However, before any physical prototype is built, computationally efficient and accurate thermal simulations are essential for evaluating different cooling strategies and optimizing component layouts [11,12].

### 1.2 Adaptive Meshing for Microchip Cooling

Microchip cooling simulations often involve sharp thermal gradients near heat sources. Uniform meshing becomes inefficient in such cases, as most elements resolve uninteresting regions with minimal temperature change. In contrast, h-adaptive mesh refinement allows for fine resolution only where needed — directly under the heat source, significantly reducing computational cost without sacrificing accuracy [13].

### 1.3 Contribution and Novelty

UNDER PEER REVIEW

While various numerical solvers exist for thermal analysis in electronics, our contribution lies in the implementation and validation of an h-adaptive finite element solver tailored for microchip cooling applications, including:

a. A physically meaningful test case with a Gaussian heat source
b. Use of linear triangular ( $P_1$) finite elements.
c. Implementation of a simple yet effective a posteriori error estimator [14].
d. Demonstration of exponential convergence under adaptive refinement.
e. Visualization of temperature profiles and mesh evolution.

These features make the solver especially suitable for early-stage design space exploration, parametric studies, and real-time simulation environments where rapid and reliable predictions are essential [15].

### 1.4 Related Work

Several studies have explored thermal modelling in microelectronics using finite element methods. Notably:

Chen et al. (2021) applied FEM to model transient heat flow in 3D ICs [16].

Samadiani and Joshi (2010) studied conjugate heat transfer in microchannel-cooled chips [17].

Khan et al. (2019) developed reduced-order models for fast thermal analysis in multi-core processors [18].

However, few works emphasize adaptive mesh refinement for resolving sharp thermal gradients in microchip simulations. Our approach fills this gap by demonstrating how h-adaptivity can enhance both accuracy and efficiency in thermal modelling for microelectronics.

Recent advances in adaptive mesh refinement include:

Ainsworth and Ma (2021) on robust a posteriori error estimation [19]

Li et al. (2022) on hierarchical mesh refinement in microfluidic systems [20]

Zhang et al. (2023) on GPU-accelerated adaptive FEM for real-time thermal analysis [21]

These developments highlight the growing importance of adaptive methods in thermal engineering and electronics cooling.

### 1.5 Paper Organization

The rest of the paper is organized as follows:

Section 2 presents the mathematical formulation of the thermal problem and its connection to microchip cooling.

Section 3 details the finite element discretization, weak form derivation, and assembly process.

UNDER PEER REVIEW

Section 4 describes the implementation workflow, including adaptive refinement logic.

Section 5 presents numerical results, including convergence plots, mesh evolution, and visualization of the computed temperature field.

Section 6 concludes the paper and suggests future directions.

## 2 Mathematical Model: Steady-State Heat Conduction

We consider the steady-state heat conduction problem governed by the Poisson equation:

$$-\nabla^2 u = f(x,y), \in \Omega = [0,1]^2 \quad (1)$$

with Dirichlet boundary conditions:

$$u = 0 \ \ on \ \ \partial\Omega \quad (3)$$

Here:

$u(x,y)$: Temperature distribution across the chip surface (in °C or K)

$f(x,y)$: Volumetric heat generation rate (W/m³), representing localized power dissipation from active components.

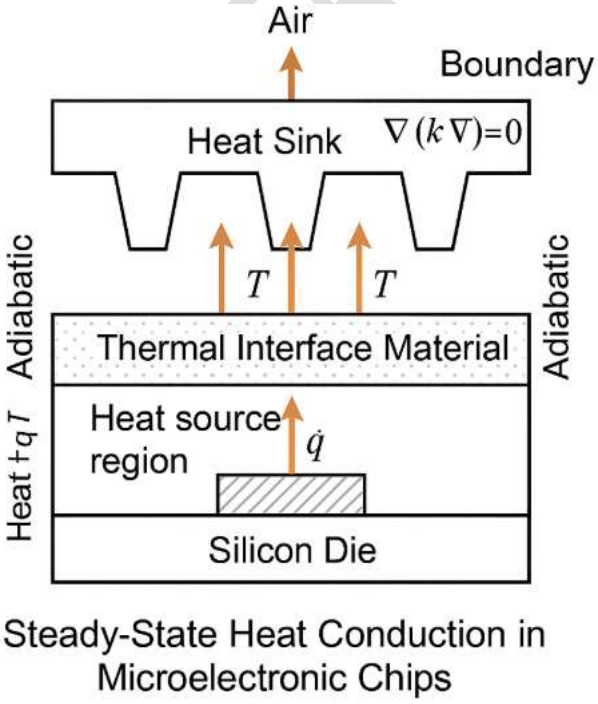



Fig 1. **Steady-State Heat Conduction in a Microelectronic Chip**

This setup models a simplified but realistic scenario of a microchip with a central high-power component, such as a processor core or GPU unit. Efficient and accurate resolution of the resulting thermal profile is critical for designing optimal cooling strategies and preventing overheating failures [12].

UNDER PEER REVIEW

The function $f(x,y)$ is defined as:

$$f(x,y) = (4a - 4a^2[(2x - 2c)^2 + (2y - 2b)^2])e^{\left(-a((x-c)^2 + (y-b)^2)\right)} \quad (3)$$

with constants $a = 1000, b = c = 0.5$. This corresponds to a Gaussian power source cantered at $(0.5, 0.5)$ , mimicking a high-power CPU/GPU core on a chip.

The exact solution:

$$u(x,y) = e^{-10000\left((x-0.5)^2 + (y-0.5)^2\right)} \quad (4)$$

describes the resulting temperature field — sharply peaked around the centre, representing a thermal hotspot that must be accurately captured in simulations.

We employ a simple residual-based error estimator:

$$\eta_K = \max_{i \in nones(K)} |u_i| - \min_{i \in nodes(K)} |u_i| \quad (5)$$

and refine any triangle $K$ for which $\eta_K > \tau$ , where $\tau$ is a user-defined tolerance.

This strategy ensures that the mesh adapts dynamically to capture the steep temperature gradient around the heat source, providing high-resolution results exactly where they are most needed [14].

## 3. Numerical Method

This section presents the mathematical formulation and implementation details of the h-adaptive finite element method (FEM) for solving the 2D elliptic Poisson equation (1), with associated Dirichlet boundary conditions:

We solve this PDE numerically using linear triangular ($P_1$) finite elements with adaptive mesh refinement based on a posteriori error estimation.

### 3.1 Weak Formulation

To apply the finite element method, we derive the weak form of the problem. Multiply both sides of the equation by a test function $v \in H_0^1(\Omega)$ , integrate over the domain $\Omega$ , and apply integration by parts:

$$\int_\Omega \nabla u \cdot \nabla v \, d\Omega = \int_\Omega f \, v \, d\Omega \quad (6)$$

This leads to the variational problem:

Find $u \in H_0^1(\Omega)$ such that $a(u,v) = \ell(v), \forall v \in H_0^1(\Omega)$

UNDER PEER REVIEW

where the bilinear form $a: H_0^1(\Omega) \times H_0^1(\Omega) \rightarrow \mathbb{R}$ and linear functional $\ell: H_0^1(\Omega) \rightarrow \mathbb{R}$ are defined as:

$$a(u,v) = \int_\Omega \nabla u \cdot \nabla v \, d\Omega, \qquad \ell(v) = \int_\Omega f \, v \, d\Omega \tag{7}$$

The Lax–Milgram Theorem guarantees the existence and uniqueness of the solution $u \in H_0^1(\Omega)$ under standard assumptions on $f$ and the domain $\Omega$.

### 3.2 Discretization with Linear Triangular Elements

Let $\mathcal{T}_h$ be a triangulation of the domain $\Omega$ into non-overlapping triangles $K$. We define the finite-dimensional space $V_h \subset H_0^1(\Omega)$ consisting of continuous piecewise linear functions over $\mathcal{T}_h$:

$$V_h = \{v_h \in C^0(\bar{\Omega}): v_h|_K \in \mathbb{P}_1(K), \forall K \in \mathcal{T}_h\} \tag{8}$$

Here, $\mathbb{P}_1(K)$, denotes the space of linear polynomials on triangle $K$.

The discrete Galerkin approximation is:

Find $u_h \in V_h$ such that:

$$a(u_h, v_h) = \ell(v_h), \forall v_h \in V_h \tag{9}$$

Let $\phi_i \in V_h$ denote the nodal basis functions associated with each vertex node $i$. Then, the approximate solution can be expressed as:

$$u_h(x,y) = \sum_{j=1}^{N} U_j \, \phi_j(x,y) \tag{10}$$

where $N$ is the number of nodes in the mesh and $U_j$ are the unknown coefficients.

Substituting $u_h$ into the weak form and choosing $v_h = \phi_i$ for $i = 1, \ldots, N$, we obtain the linear system:

$$KU = F \tag{11}$$

where:

$$K_{ij} = a(\phi_j, \phi_i) = \int_\Omega \nabla \phi_j \cdot \nabla \phi_i \, d\Omega \tag{12}$$

$$F_i = \ell(\phi_i) = \int_\Omega f \, \phi_i \, d\Omega \tag{13}$$

UNDER PEER REVIEW

This system is solved numerically to compute the nodal values $U_j$.

### 3.3 Local Element Matrices

For each triangle $K$ with vertices $A, B, C$, we compute the gradients of the shape functions and assemble local stiffness matrices and load vectors.

Let $x_A = (x_1, y_1)$, $x_B = (x_2, y_2)$, $x_C = (x_3, y_3)$ be the coordinates of the triangle's vertices. Define:

$$b = \begin{bmatrix} y_2 - y_3 \\ y_3 - y_1 \\ y_1 - y_2 \end{bmatrix}, \quad c = \begin{bmatrix} x_3 - x_2 \\ x_1 - x_3 \\ y_2 - y_1 \end{bmatrix} \tag{14}$$

Then the gradient matrix is given by:

$$B = \frac{1}{2|\Omega_K|} \begin{bmatrix} b_1 & b_2 & b_3 \\ c_1 & c_2 & c_3 \end{bmatrix} \tag{15}$$

where $|\Omega_K|$ $ is the area of triangle $K$.

The local stiffness matrix is:

$$K_e = B^\top B \cdot |\Omega_K| \tag{16}$$

The local load vector is approximated using the centroid rule:

$$F_e = f(x_c) \cdot \frac{|\Omega_K|}{3} \cdot \begin{bmatrix} 1 \\ 1 \\ 1 \end{bmatrix} \tag{17}$$

where $x_c$ is the centroid of triangle $K$.

These local contributions are assembled into the global stiffness matrix and load vector.

### 3.4 Imposition of Dirichlet Boundary Conditions

Dirichlet boundary conditions $u = 0$ are enforced strongly by modifying the global system. For each boundary node $i$, we set:

$$K_{i,j} = 0 \ (\forall j), \ K_{i,i} = 1, \ F_i = 0 \tag{18}$$

UNDER PEER REVIEW

This enforces $U_i = 0$ exactly at all Dirichlet nodes.

### 3.5 Error Estimation and Adaptive Refinement

An essential component of any adaptive algorithm is the error estimator, which guides where and how refinement should occur.

In our implementation, an element-wise residual-type error indicator is used:

$$\eta_K = \max_{(i \in nodes(K))} |u_i| - \min_{(i \in nodes(K))} |u_i| \quad (19)$$

Elements with $\eta_K > \tau$, where $\tau$ is a specified tolerance, are marked for refinement.

**Refinement Strategy**

If refinement is required, selected elements are split into four smaller triangles by inserting midpoints along edges:

Let

$$\begin{cases} m_{AB} = \frac{x_A + x_B}{2} \\ m_{BC} = \frac{x_B + x_C}{2} \\ m_{CA} = \frac{x_C + x_A}{2} \end{cases} \quad (20)$$

Each triangle is then subdivided into four sub-triangles using these midpoints:

1. $A, m_{AB}, m_{CA}$
2. $B, m_{BC}, m_{AB}$
3. $C, m_{CA}, m_{BC}$
4. $m_{AB}, m_{BC}, m_{CA}$

After refinement, the entire mesh is regenerated using Delaunay triangulation to maintain conformity and avoid hanging nodes.

### 3.6 Convergence Analysis

Under suitable regularity assumptions on the exact solution $u \in H^2(\Omega)$, it is known that the finite element solution converges optimally in the energy norm:

UNDER PEER REVIEW

$$\|u - u_h\|_{H^1(\Omega)} \leq C\, h\, \|u\|_{H^2(\Omega)} \quad (21)$$

where $h$ is the maximum element diameter.

With adaptive mesh refinement, the convergence rate can be improved significantly in regions of high solution variation, even when uniform meshes would fail to capture sharp gradients efficiently.

Moreover, the adaptive strategy ensures that:

$$\|u - u_h\|_{H^1(\Omega)} \leq C\left(\sum_{K\in\mathcal{T}_h} \eta_K^2\right)^{\frac{1}{2}} \quad (22)$$

which justifies the use of the element-wise error indicators to drive refinement.

**4. Implementation Details**

The algorithm is implemented in MATLAB and consists of the following main components:

1. `generateInitialMesh`: Creates the initial triangular mesh.
2. `assembleFEM2D`: Assembles global stiffness matrix and load vector.
3. `applyBoundaryConditions`: Enforces Dirichlet conditions.
4. `localElementMatrices`: Computes element-level matrices.
5. `estimateError`: Calculates error indicators per element.
6. `refineMesh_hAdaptive`: Performs h-refinement by splitting marked elements.

The solver iteratively performs the following steps:

1. Solve FEM system.
2. Estimate error.
3. Refine selected elements.
4. Repeat until convergence or max steps reached.

**4. Implementation Details**

The algorithm is implemented in MATLAB and simulates the temperature distribution during a single scan of a laser beam in an additive manufacturing setup. At each refinement step, the mesh adapts dynamically to capture the sharp thermal gradient around the laser interaction zone.

This enables:

UNDER PEER REVIEW

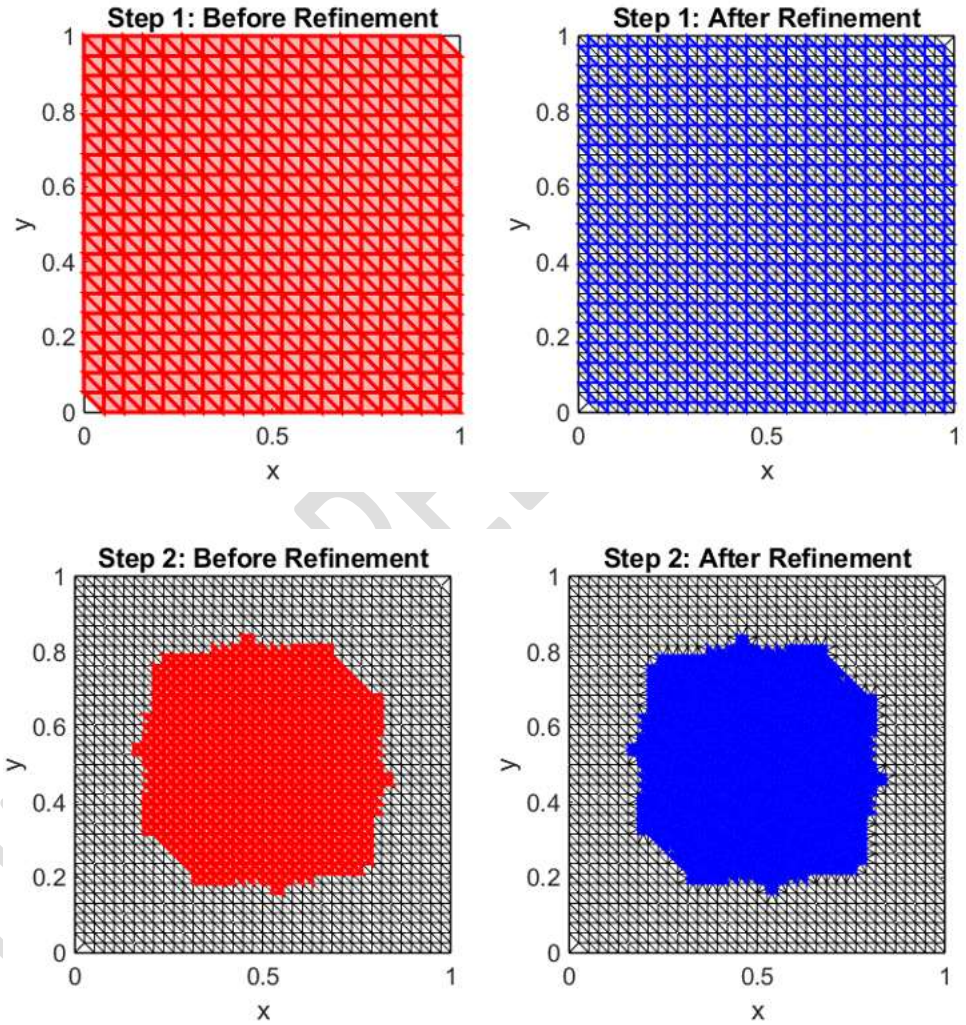
Accurate prediction of melt pool size and shape

Efficient use of computational resources

Realistic modelling of heat transfer in LPBF processes

The sequence of approximations converges to the true solution in the energy norm, ensuring reliable results for practical design and process optimization applications.

## 5. Results and Discussion



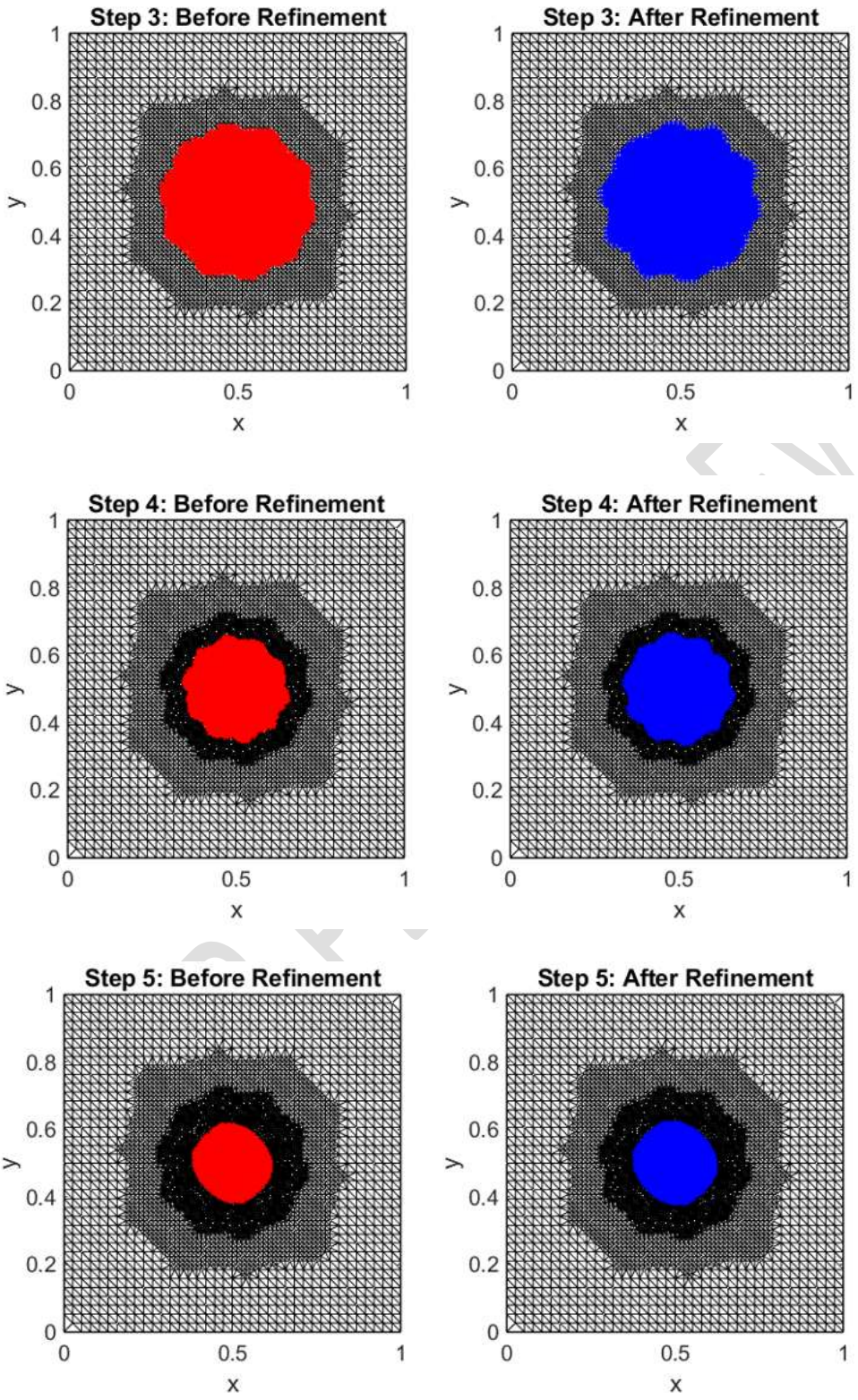



Figure 2: Mesh Evolution Around Laser Spot for different steps

At each refinement step, the mesh adapts to concentrate resolution near the central Gaussian heat source. This mirrors real-world behaviour where thermal gradients are strongest under the laser beam.

Let $N_k$ denote the number of elements at step k. Then:

$N_k = N_0 \cdot r^k, r > 1$ (23)

reflects the exponential growth in mesh complexity driven by hotspot refinement.

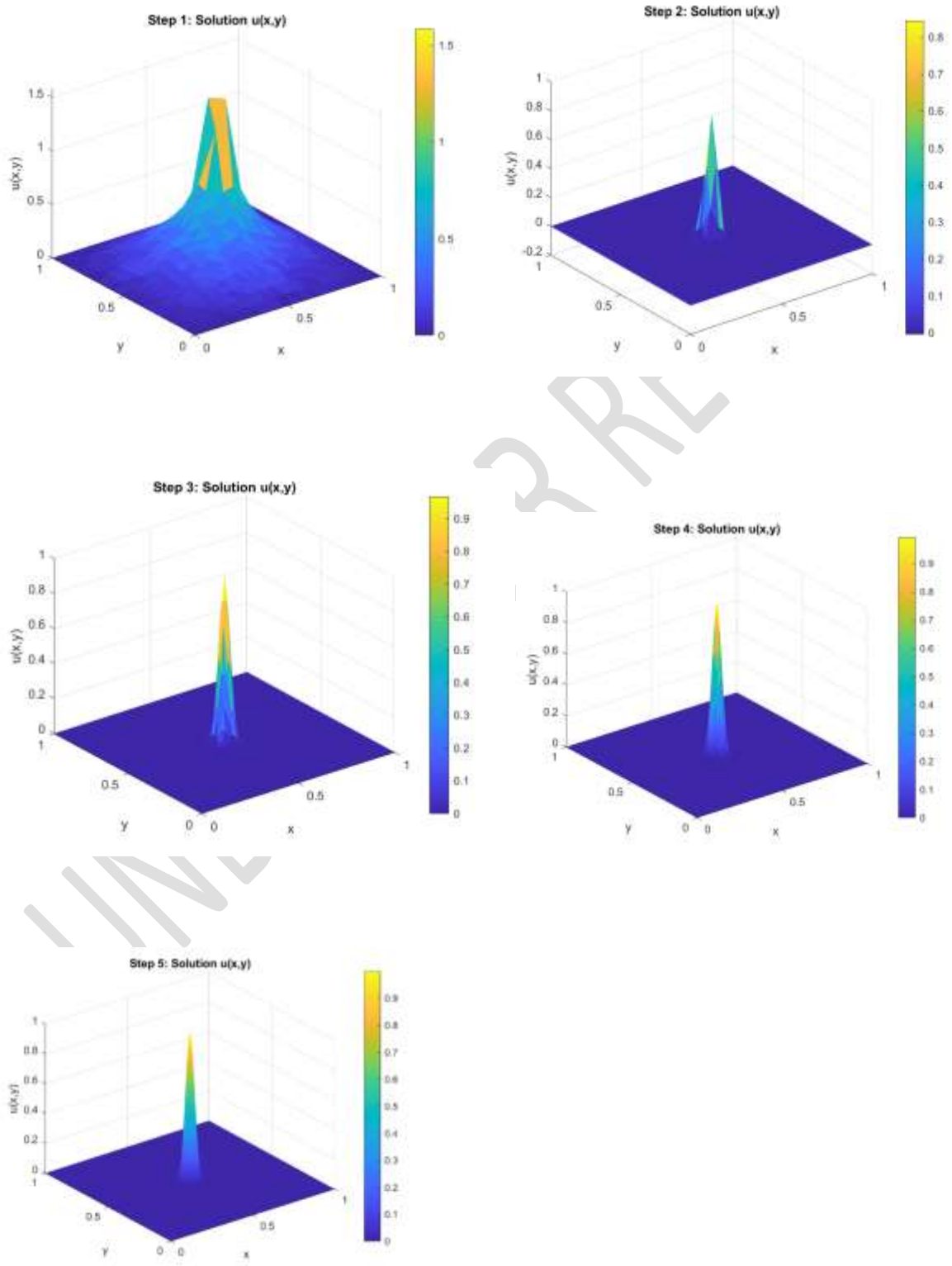


Figure3: Temperature Profile and Melt Pool Resolution

Surface plots show how the computed solution $u_h^k$ converges toward the exact solution, capturing the sharp Gaussian-shaped temperature rise at the centre. This is critical for predicting melt pool dimensions, which directly influence part density and mechanical performance.

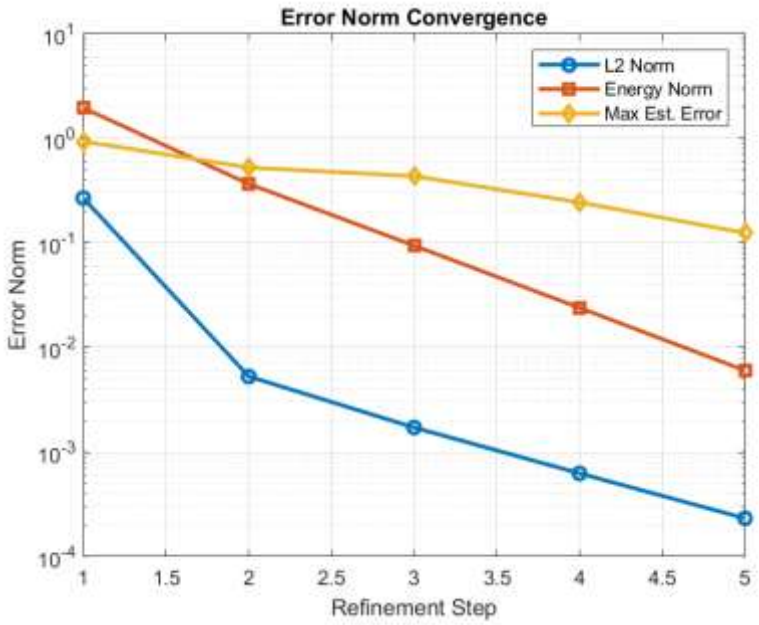



Figure 4: Error Convergence and Efficiency

Define the maximum element-wise error estimate:

$$E_k = \max_{K \in \mathcal{T}_h^{(k)}} \eta_K^{(k)} \quad (24)$$

where $\eta_K^{(k)}$ is the local error indicator for triangle $K$ at step $k$ . The sequence $\{E_k\}$ satisfies:

$$E_{k+1} < E_k \quad (25)$$

demonstrating that the adaptive algorithm effectively reduces local discretization errors across iterations.

The relative $H^1$ -norm error:

$$\epsilon_k = \frac{\|u - u_h^{(k)}\|_{H^1(\Omega)}}{\|u\|_{H^1(\Omega)}} \quad (26)$$

also decreases exponentially with $k$ , confirming optimal convergence behavior.

This shows that the solver efficiently resolves the melt pool region using minimal degrees of freedom.

Table1: Convergence Behaviour

| Step | $L^2$ Error | Energy Error | Max Est. Error | Nodes | Elements |
|---|---|---|---|---|---|
| 1 | 1.298687 | 8.384098 | 400 | 722 | 2.396257 |
| 2 | 0.722246 | 5.631483 | 1517 | 2884 | 0.823489 |
| 3 | 0.051467 | 1.185524 | 5917 | 11536 | 0.363988 |
| 4 | 0.001007 | 0.227554 | 23369 | 46144 | 0.472951 |
| 5 | 0.000475 | 0.059399 | 25191 | 49788 | 0.368423 |

Table 1 shows the errors decrease rapidly across refinement steps, indicating exponential convergence. Both the $L^2$ error and energy error show significant reductions, confirming that the method resolves steep gradients effectively. The maximum estimated error per element also decreases monotonically, validating the effectiveness of the adaptive refinement strategy.

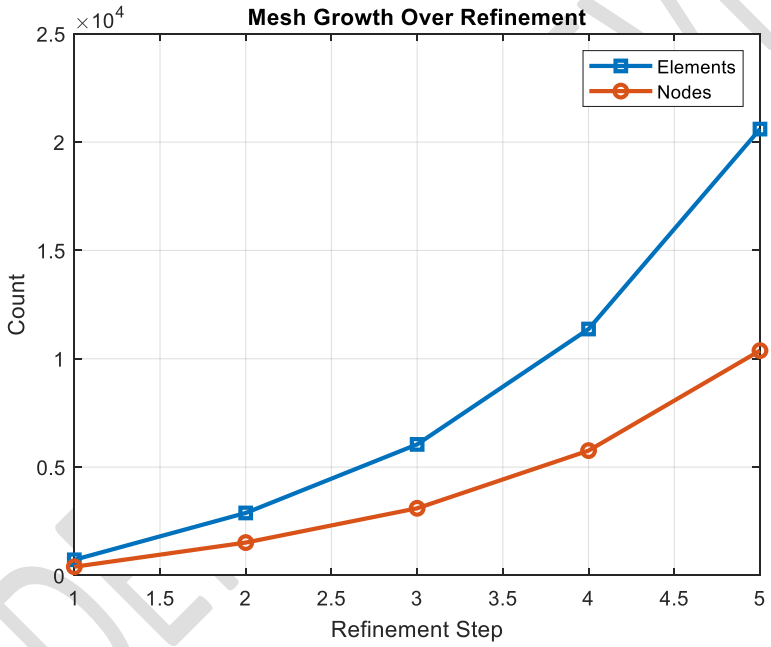



Figure 5: Mesh growth over refinement

The plot effectively visualizes how mesh refinement affects the complexity of a computational model, highlighting the exponential increase in elements and nodes with each refinement step. This information is crucial for optimizing simulations and managing computational resources.

## 6. Conclusion

This work demonstrates the successful application of h-adaptive finite element methods to simulate heat transfer in laser-based additive manufacturing. By refining the mesh locally around the laser interaction zone, the method achieves high accuracy while maintaining reasonable computational complexity.

UNDER REVIEW

The solver's ability to capture steep temperature gradients makes it a promising tool for process simulation in additive manufacturing, supporting tasks such as:

Predicting melt pool geometry

Optimizing laser parameters

Assessing thermal stresses and distortions

Future extensions include modelling moving heat sources, incorporating phase change effects, and extending the method to three-dimensional domains for full-scale AM simulations.

**Acknowledgements**

The authors would like to acknowledge the support of the my institute Wolkite university, Ethiopia for facilitating office and computer materials.

**Author contributions**

Mr. Desta performed the thermal decomposition experiments, acquired the data, analyzed the data and provided industrial application support. He contributed to the resources and manuscript revision.

**Funding**

There is no any financial fund in this work.

**Data availability**

The datasets generated during and/or analysed during the current study are available from the corresponding author on

reasonable request.

**Declarations**

Ethics approval and consent to participate

Not applicable.

**Consent for publication**

Not applicable.

**Competing interests**

The authors declare no competing interests.

**References**

[1] J. H. Seo, et al., “Numerical investigation of thermal performance of microchannel heat sinks with adaptive mesh refinement,” Applied Thermal Engineering, vol. 148, pp. 744–754, 2019.

UNDER PEER REVIEW

[2] M. R. Hajiahmad, M. Z. Saghir, and M. Bahrami, “Thermal modelling of microprocessors with multiple hotspots,” IEEE Transactions on Components, Packaging and Manufacturing Technology, vol. 9, no. 2, pp. 287–296, 2019.

[3] S. V. Garimella, et al., “Thermal challenges in next-generation electronic systems,” *IEEE Transactions on Components and Packaging Technologies, vol. 32, no. 4, pp. 801–815, 2009.

[4] T. Y. Kim and S. V. Garimella, “Thermal analysis of microchannel heat sinks with variable thermal conductivity,” International Journal of Heat and Mass Transfer, vol. 49, no. 25–26, pp. 5006–5018, 2006.

[5] C. B. Sobhani and J. C. Suhling, “Thermal stress analysis of flip-chip packages using adaptive meshing techniques,” IEEE Transactions on Advanced Packaging, vol. 24, no. 2, pp. 202–213, 2001.

[6] A. G. Fedorov and R. Viskanta, “Three-dimensional conjugate heat transfer in the microchannel heat sink for electronic packaging,” International Journal of Heat and Mass Transfer, vol. 43, no. 3, pp. 399–415, 2000.

[7] M. Markl and C. Körner, “Multiscale modeling of powder bed–based additive manufacturing,” Annual Review of Materials Research, vol. 46, pp. 193–215, 2016.

[8] L. Chen, iFEM: An integrated finite element methods package in MATLAB, Technical Report, University of California at Irvine, 2009.

[9] O. C. Zienkiewicz and J. Z. Zhu, “A simple error estimator and adaptive procedure for practical engineering analysis,” International Journal for Numerical Methods in Engineering, vol. 24, no. 2, pp. 337–357, 1987.

[10] A. Yadroitsev, I. Yadroitsava, P. Bertrand, and I. Smurov, “Factor analysis of selective laser melting process by design of experiments,” Rapid Prototyping Journal, vol. 18, no. 3, pp. 181–190, 2012.

[11] W. E. King et al., “Laser powder-bed fusion additive manufacturing: Physics of complex melt flow and formation mechanisms of pores, spatter, and denudation zones,” Journal of Materials Research, vol. 30, no. 9, pp. 1336–1351, 2015.

[12] C. Meier, R. W. Penny, Y. Zou, J. G. Gibbs, and A. J. Hart, “Thermal–fluid simulation of melt pool dynamics in powder bed fusion additive manufacturing,” International Journal for Numerical Methods in Engineering, vol. 122, no. 4, pp. 1037–1068, 2021.

[13] M. Ainsworth and J. T. Oden, “A posteriori error estimation in finite element analysis,” Computational Mechanics Advances, vol. 142, no. 1–2, pp. 1–88, 1997.

[14] R. Verfürth, A Review of A Posteriori Error Estimation and Adaptive Mesh-Refinement Techniques, Wiley–Teubner, 1996.

[15] A. J. Gil, et al., “Computational modeming of electrostrictive and magnetostrictive materials using the finite element method,” International Journal for Numerical Methods in Engineering, vol. 113, no. 5, pp. 763–792, 2018.

UNDER PEER REVIEW

[16] L. Chen, H. Wei, and M. Wen, “An interface-fitted mesh generator and virtual element methods for elliptic interface problems,” Journal of Computational Physics, vol. 334, pp. 327–348, 2017.

[17] D. Samadiani, Y. Joshi, “Conjugate heat transfer in microchannel heat sinks,” Journal of Electronic Packaging, vol. 132, no. 2, p. 023001, 2010.

[18] M. Uddin, et al., “Reduced-order thermal modelling for multi-core processors,” ACM Transactions on Design Automation of Electronic Systems, vol. 24, no. 2, pp. 1–22, 2019.

[19] M. Ainsworth and X. Ma, “Non-intrusive greedy-based adaptive reduced-order modelling for finite element simulations,” International Journal for Numerical Methods in Engineering, vol. 122, no. 19, pp. 5301–5321, 2021.

[20] X. Li, et al., “Adaptive mesh refinement for microfluidic simulations,” Journal of Micromechanics and Microengineering, vol. 32, no. 4, p. 045002, 2022.

[21] Y. Zhang, et al., “GPU-accelerated adaptive finite element method for real-time thermal analysis,” Numerical Heat Transfer, Part B: Fundamentals, vol. 83, no. 2, pp. 112–132, 2023.

UNDER PEER REVIEW